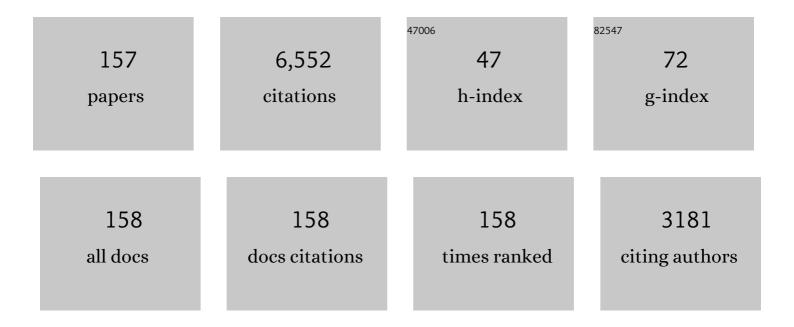
Louise Olsson

List of Publications by Year in descending order

Source: https://exaly.com/author-pdf/6371192/publications.pdf Version: 2024-02-01



#	Article	IF	CITATIONS
1	The Effect of Si/Al Ratio on the Oxidation and Sulfur Resistance of Beta Zeolite-Supported Pt and Pd as Diesel Oxidation Catalysts. ACS Engineering Au, 2022, 2, 27-45.	5.1	11
2	Kinetic modeling of CO assisted passive NOx adsorption on Pd/SSZ-13. Chemical Engineering Journal, 2022, 428, 132459.	12.7	17
3	Methanol mediated direct CO2 hydrogenation to hydrocarbons: Experimental and kinetic modeling study. Chemical Engineering Journal, 2022, 435, 135090.	12.7	22
4	Advantages of High-Siliceous Zeolites in the Reactivity and Stability of Diesel Oxidation Catalysts. ACS Engineering Au, 2022, 2, 219-235.	5.1	8
5	Elucidating the role of NiMoS-USY during the hydrotreatment of Kraft lignin. Chemical Engineering Journal, 2022, 442, 136216.	12.7	14
6	Deactivation of phosphorus-poisoned Pd/SSZ-13 for the passive adsorption of NOx. Journal of Environmental Chemical Engineering, 2022, 10, 107608.	6.7	8
7	Insight into CO induced degradation mode of Pd/SSZ-13 in NOx adsorption and release: Experiment and modeling. Chemical Engineering Journal, 2022, 439, 135714.	12.7	13
8	<i>In situ</i> DRIFT studies on N ₂ O formation over Cu-functionalized zeolites during ammonia-SCR. Catalysis Science and Technology, 2022, 12, 3921-3936.	4.1	4
9	The effect of Pt/Pd ratio on the oxidation activity and resistance to sulfur poisoning for Pt-Pd/BEA diesel oxidation catalysts with high siliceous content. Journal of Environmental Chemical Engineering, 2022, 10, 108217.	6.7	13
10	Layered Pd/SSZ-13 with Cu/SSZ-13 as PNA â~' SCR dual-layer monolith catalyst for NOx abatement. Catalysis Today, 2021, 360, 356-366.	4.4	20
11	The role of catalyst poisons during hydrodeoxygenation of renewable oils. Catalysis Today, 2021, 367, 28-42.	4.4	16
12	Role of transition metals on MoS ₂ -based supported catalysts for hydrodeoxygenation (HDO) of propylguaiacol. Sustainable Energy and Fuels, 2021, 5, 2097-2113.	4.9	19
13	Hydrotreatment of lignin dimers over NiMoS-USY: effect of silica/alumina ratio. Sustainable Energy and Fuels, 2021, 5, 3445-3457.	4.9	21
14	The role of Pd–Pt Interactions in the Oxidation and Sulfur Resistance of Bimetallic Pd–Pt/γ-Al ₂ O ₃ Diesel Oxidation Catalysts. Industrial & Engineering Chemistry Research, 2021, 60, 6596-6612.	3.7	33
15	The Impact of Lanthanum and Zeolite Structure on Hydrocarbon Storage. Catalysts, 2021, 11, 635.	3.5	7
16	Characterization Method for Gas Flow Reactor Experiments—NH3 Adsorption on Vanadium-Based SCR Catalysts. Industrial & Engineering Chemistry Research, 2021, 60, 11399-11411.	3.7	3
17	The Promotor and Poison Effects of the Inorganic Elements of Kraft Lignin during Hydrotreatment over NiMoS Catalyst. Catalysts, 2021, 11, 874.	3.5	9
18	Impact of Different Synthesis Methods on the Low-Temperature Deactivation of Cu/SAPO-34 for NH3-SCR Reaction. Emission Control Science and Technology, 2021, 7, 198-209.	1.5	5

#	Article	IF	CITATIONS
19	Reductive liquefaction of lignin to monocyclic hydrocarbons: ReS2/Al2O3 as efficient char inhibitor and hydrodeoxygenation catalyst. Applied Catalysis B: Environmental, 2021, 297, 120449.	20.2	20
20	Regeneration of sulfur-poisoned Cu-SSZ-13 catalysts: Copper speciation and catalytic performance evaluation. Applied Catalysis B: Environmental, 2021, 299, 120626.	20.2	21
21	Recent advances in hydrogenation of CO ₂ into hydrocarbons <i>via</i> methanol intermediate over heterogeneous catalysts. Catalysis Science and Technology, 2021, 11, 1665-1697.	4.1	64
22	Thermal annealing effects on hydrothermally synthesized unsupported MoS ₂ for enhanced deoxygenation of propylguaiacol and kraft lignin. Sustainable Energy and Fuels, 2021, 5, 5270-5286.	4.9	12
23	Comparative Study of SO2 and SO2/SO3 Poisoning and Regeneration of Cu/BEA and Cu/SSZ-13 for NH3 SCR. Emission Control Science and Technology, 2021, 7, 232-246.	1.5	12
24	Structure and performance of zeolite supported Pd for complete methane oxidation. Catalysis Today, 2021, 382, 3-12.	4.4	24
25	N ₂ O Formation during NH ₃ -SCR over Different Zeolite Frameworks: Effect of Framework Structure, Copper Species, and Water. Industrial & Engineering Chemistry Research, 2021, 60, 17826-17839.	3.7	24
26	Global Kinetic Model of a Three-Way-Catalyst-Coated Gasoline Particulate Filter: Catalytic Effects of Soot Accumulation. Industrial & Engineering Chemistry Research, 2021, 60, 16899-16910.	3.7	2
27	NiMoS on alumina-USY zeolites for hydrotreating lignin dimers: effect of support acidity and cleavage of C–C bonds. Sustainable Energy and Fuels, 2020, 4, 149-163.	4.9	21
28	Insight into hydrothermal aging effect on Pd sites over Pd/LTA and Pd/SSZ-13 as PNA and CO oxidation monolith catalysts. Applied Catalysis B: Environmental, 2020, 278, 119315.	20.2	45
29	A deactivation mechanism study of phosphorus-poisoned diesel oxidation catalysts: model and supplier catalysts. Catalysis Science and Technology, 2020, 10, 5602-5617.	4.1	16
30	Effects of Feed Gas Composition on Fresh and Aged TWC-Coated GPFs Loaded with Real Soot. Industrial & Engineering Chemistry Research, 2020, 59, 10790-10803.	3.7	8
31	Hydrothermal Aging of Pd/LTA Monolithic Catalyst for Complete CH4 Oxidation. Catalysts, 2020, 10, 517.	3.5	12
32	Regeneration of Cu/SAPO-34(MO) with H ₂ O only: too good to be true?. Catalysis Science and Technology, 2020, 10, 1529-1538.	4.1	12
33	Regeneration of water-deactivated Cu/SAPO-34(MO) with acids. Catalysis Science and Technology, 2020, 10, 1539-1550.	4.1	11
34	Deactivation mechanism of Cu active sites in Cu/SSZ-13 — Phosphorus poisoning and the effect of hydrothermal aging. Applied Catalysis B: Environmental, 2020, 269, 118781.	20.2	45
35	Influencing the NO _x Stability by Metal Oxide Addition to Pd/BEA for Passive NO _x Adsorbers. Industrial & Engineering Chemistry Research, 2020, 59, 9830-9840.	3.7	19
36	Insight into the SO2 poisoning mechanism for NOx removal by NH3-SCR over Cu/LTA and Cu/SSZ-13. Chemical Engineering Journal, 2020, 395, 125048.	12.7	44

#	Article	IF	CITATIONS
37	Zeolite Beta Doped with La, Fe, and Pd as a Hydrocarbon Trap. Catalysts, 2020, 10, 173.	3.5	8
38	The impact of automotive catalysis on the United Nations sustainable development goals. Nature Catalysis, 2019, 2, 566-570.	34.4	81
39	Kinetic study of hydrodeoxygenation of stearic acid as model compound for renewable oils. Chemical Engineering Journal, 2019, 364, 376-389.	12.7	44
40	Sulfur Poisoning Effects on Modern Lean NOx Trap Catalysts Components. Catalysts, 2019, 9, 492.	3.5	6
41	Deactivation of Cu-SSZ-13 SCR catalysts by vapor-phase phosphorus exposure. Applied Catalysis B: Environmental, 2019, 256, 117815.	20.2	36
42	Understanding the mechanism of low temperature deactivation of Cu/SAPO-34 exposed to various amounts of water vapor in the NH3-SCR reaction. Catalysis Science and Technology, 2019, 9, 3623-3636.	4.1	22
43	Lean and rich aging of a Cu/SSZ-13 catalyst for combined lean NO _x trap (LNT) and selective catalytic reduction (SCR) concept. Catalysis Science and Technology, 2019, 9, 2152-2162.	4.1	16
44	The effect of Si/Al ratio of zeolite supported Pd for complete CH4 oxidation in the presence of water vapor and SO2. Applied Catalysis B: Environmental, 2019, 250, 117-131.	20.2	96
45	Hydroconversion of abietic acid into value-added fuel components over sulfided NiMo catalysts with varying support acidity. Fuel Processing Technology, 2019, 190, 55-66.	7.2	15
46	Influence of H2, CO, C3H6, and C7H8 as Reductants on DeNOx Behavior of Dual Monoliths for NOx Storage/Reduction Coupled with Selective Catalytic Reduction. Industrial & Engineering Chemistry Research, 2019, 58, 7001-7013.	3.7	11
47	Catalytic hydrotreatment of pyrolysis oil phenolic compounds over Pt/Al2O3 and Pd/C. Fuel, 2019, 243, 441-448.	6.4	20
48	Deactivation of Cu/SSZ-13 NH3-SCR Catalyst by Exposure to CO, H2, and C3H6. Catalysts, 2019, 9, 929.	3.5	6
49	A kinetic model for SCR coated particulate filters—Effect of ammonia-soot interactions. Applied Catalysis B: Environmental, 2019, 241, 66-80.	20.2	14
50	Insights into hydrothermal aging of phosphorus-poisoned Cu-SSZ-13 for NH3-SCR. Applied Catalysis B: Environmental, 2019, 241, 205-216.	20.2	84
51	Volatilisation and subsequent deposition of platinum oxides from diesel oxidation catalysts. Applied Catalysis B: Environmental, 2019, 241, 338-350.	20.2	24
52	Chemical poisoning by zinc and phosphorous of Pt/Ba/Al2O3 NOx storage catalysts. Applied Catalysis A: General, 2019, 571, 158-169.	4.3	2
53	Investigation of the robust hydrothermal stability of Cu/LTA for NH3-SCR reaction. Applied Catalysis B: Environmental, 2019, 246, 242-253.	20.2	73
54	The effect of rosin acid on hydrodeoxygenation of fatty acid. Journal of Energy Chemistry, 2019, 28, 85-94.	12.9	13

#	Article	IF	CITATIONS
55	Trade-off between NOx storage capacity and sulfur tolerance on Al2O3/ZrO2/TiO2–based DeNOx catalysts. Catalysis Today, 2019, 320, 152-164.	4.4	7
56	Complete methane oxidation over Ba modified Pd/Al2O3: The effect of water vapor. Applied Catalysis B: Environmental, 2018, 231, 242-250.	20.2	53
57	Investigating the effect of Fe as a poison for catalytic HDO over sulfided NiMo alumina catalysts. Applied Catalysis B: Environmental, 2018, 227, 240-251.	20.2	66
58	Mechanistic study of hydrothermally aged Cu/SSZ-13 catalysts for ammonia-SCR. Catalysis Today, 2018, 307, 55-64.	4.4	56
59	The effect of changing the gas composition on soot oxidation over DPF and SCR-coated filters. Catalysis Today, 2018, 306, 243-250.	4.4	23
60	The addition of alkali and alkaline earth metals to Pd/Al2O3 to promote methane combustion. Effect of Pd and Ca loading. Catalysis Today, 2018, 299, 212-218.	4.4	21
61	Influence of Bio-Oil Phospholipid on the Hydrodeoxygenation Activity of NiMoS/Al2O3 Catalyst. Catalysts, 2018, 8, 418.	3.5	14
62	Gas-Phase Phosphorous Poisoning of a Pt/Ba/Al2O3 NOx Storage Catalyst. Catalysts, 2018, 8, 155.	3.5	6
63	Deceleration of SO2 poisoning on PtPd/Al2O3 catalyst during complete methane oxidation. Applied Catalysis B: Environmental, 2018, 236, 384-395.	20.2	51
64	Effect of various structure directing agents (SDAs) on low-temperature deactivation of Cu/SAPO-34 during NH ₃ -SCR reaction. Catalysis Science and Technology, 2018, 8, 3090-3106.	4.1	40
65	Detailed Characterization Studies of Vehicle and Rapid Aged Commercial Lean NO _{<i>x</i>} Trap Catalysts. Industrial & Engineering Chemistry Research, 2018, 57, 9362-9373.	3.7	7
66	The Effect of Si/Al Ratio for Pd/BEA and Pd/SSZ-13 Used as Passive NOx Adsorbers. Topics in Catalysis, 2018, 61, 2007-2020.	2.8	48
67	Micro-calorimetric studies of NO2 adsorption on Pt/BaO-supported on γ-Al2O3 NOx storage and reduction (NSR) catalysts—Impact of CO2. Molecular Catalysis, 2017, 436, 43-52.	2.0	9
68	Effect of Dimethyl Disulfide on Activity of NiMo Based Catalysts Used in Hydrodeoxygenation of Oleic Acid. Industrial & Engineering Chemistry Research, 2017, 56, 5547-5557.	3.7	23
69	The effect of water on methane oxidation over Pd/Al ₂ O ₃ under lean, stoichiometric and rich conditions. Catalysis Science and Technology, 2017, 7, 3084-3096.	4.1	51
70	Ammonia Desorption Peaks Can Be Assigned to Different Copper Sites in Cu/SSZ-13. Catalysis Letters, 2017, 147, 1882-1890.	2.6	68
71	Influence of phosphorus on Cu-SSZ-13 for selective catalytic reduction of NO x by ammonia. Catalysis Today, 2017, 297, 46-52.	4.4	35
72	Effect of gas compositions on SO2 poisoning over Cu/SSZ-13 used for NH3-SCR. Applied Catalysis B: Environmental, 2017, 219, 142-154.	20.2	85

#	Article	IF	CITATIONS
73	An Experimental and Kinetic Modelling Study for Methane Oxidation over Pd-based Catalyst: Inhibition by Water. Catalysis Letters, 2017, 147, 2360-2371.	2.6	24
74	The influence of gas composition on Pd-based catalyst activity in methane oxidation â^' inhibition and promotion by NO. Applied Catalysis B: Environmental, 2017, 200, 351-360.	20.2	53
75	Sulfur-tolerant BaO/ZrO ₂ /TiO ₂ /Al ₂ O ₃ quaternary mixed oxides for deNO _X catalysis. Catalysis Science and Technology, 2017, 7, 133-144.	4.1	8
76	Impact of Copper Loading on NH3-Selective Catalytic Reduction, Oxidation Reactions and N2O Formation over Cu/SAPO-34. Energies, 2017, 10, 489.	3.1	30
77	Mechanistic Investigation of the Reduction of NOx over Pt- and Rh-Based LNT Catalysts. Catalysts, 2016, 6, 46.	3.5	11
78	Adsorption and Oxidation Investigations over Pt/Al2O3 Catalyst: A Microcalorimetric Study. Catalysts, 2016, 6, 73.	3.5	6
79	Selective oxidation of ammonia to nitrogen on bi-functional Cu–SSZ-13 and Pt/Al2O3 monolith catalyst. Catalysis Today, 2016, 267, 130-144.	4.4	52
80	Deactivation of Cu-SSZ-13 by SO ₂ exposure under SCR conditions. Catalysis Science and Technology, 2016, 6, 2565-2579.	4.1	95
81	The effect of soot on ammonium nitrate species and NO 2 selective catalytic reduction over Cu–zeolite catalyst-coated particulate filter. Philosophical Transactions Series A, Mathematical, Physical, and Engineering Sciences, 2016, 374, 20150086.	3.4	11
82	A kinetic model for sulfur poisoning and regeneration of Cu/SSZ-13 used for NH 3 -SCR. Applied Catalysis B: Environmental, 2016, 183, 394-406.	20.2	60
83	The effect of iron loading and hydrothermal aging on one-pot synthesized Fe/SAPO-34 for ammonia SCR. Applied Catalysis B: Environmental, 2016, 180, 775-787.	20.2	68
84	Evaluation of an Integrated Selective Catalytic Reduction-Coated Particulate Filter. Industrial & Engineering Chemistry Research, 2015, 54, 11779-11791.	3.7	22
85	Effect of Thermal Treatment on Hydrogen Uptake and Characteristics of Ni-, Co-, and Mo-Containing Catalysts. Industrial & Engineering Chemistry Research, 2015, 54, 11511-11524.	3.7	12
86	Stability and activity of Pd-, Pt- and Pd–Pt catalysts supported on alumina for NO oxidation. Applied Catalysis B: Environmental, 2015, 168-169, 342-352.	20.2	87
87	Evaluation of H2 effect on NO oxidation over a diesel oxidation catalyst. Applied Catalysis B: Environmental, 2015, 179, 542-550.	20.2	20
88	Comparison of Cu/BEA, Cu/SSZ-13 and Cu/SAPO-34 for ammonia-SCR reactions. Catalysis Today, 2015, 258, 49-55.	4.4	103
89	A multi-site kinetic model for NH3-SCR over Cu/SSZ-13. Applied Catalysis B: Environmental, 2015, 174-175, 212-224.	20.2	110
90	NH3-SCR Activity of H-BEA and Fe-BEA After Potassium Exposure. Topics in Catalysis, 2015, 58, 1012-1018.	2.8	3

#	Article	IF	CITATIONS
91	Deactivation mechanisms of iron-exchanged zeolites for NH3-SCR applications. Catalysis Today, 2015, 258, 432-440.	4.4	12
92	Kinetic modeling of Feâ€BEA as NH ₃ â€SCR catalyst—effect of phosphorous. AICHE Journal, 2015, 61, 215-223.	3.6	10
93	Impact of sulfur oxide on NH3-SCR over Cu-SAPO-34. Applied Catalysis B: Environmental, 2015, 166-167, 568-579.	20.2	111
94	Chemical deactivation of H-BEA and Fe-BEA as NH3-SCR catalysts—effect of potassium. Applied Catalysis B: Environmental, 2015, 166-167, 277-286.	20.2	33
95	Deactivation of Cu/SAPO-34 during low-temperature NH3-SCR. Applied Catalysis B: Environmental, 2015, 165, 192-199.	20.2	92
96	Global kinetic modeling of hydrothermal aging of NH3-SCR over Cu-zeolites. Applied Catalysis B: Environmental, 2015, 163, 382-392.	20.2	46
97	Kinetic modeling of NH3-SCR over a supported Cu zeolite catalyst using axial species distribution measurements. Applied Catalysis B: Environmental, 2015, 163, 393-403.	20.2	35
98	Chemical deactivation of Fe-BEA as NH3-SCR catalyst—Effect of phosphorous. Applied Catalysis B: Environmental, 2014, 147, 111-123.	20.2	54
99	Silver as Storage Compound for NOx at Low Temperatures. Catalysis Letters, 2014, 144, 674-684.	2.6	27
100	Effect of Enhanced Support Acidity on the Sulfate Storage and the Activity of Pt/γ-Al2O3 for NO Oxidation and Propylene Oxidation. Catalysis Letters, 2014, 144, 22-31.	2.6	8
101	The Effect of NO2/NO x Feed Ratio on the NH3-SCR System Over Cu–Zeolites with Varying Copper Loading. Catalysis Letters, 2014, 144, 70-80.	2.6	23
102	The effect of Cu-loading on different reactions involved in NH3-SCR over Cu-BEA catalysts. Journal of Catalysis, 2014, 311, 170-181.	6.2	91
103	Effect of post-synthesis hydrogen-treatment on the nature of iron species in Fe-BEA as NH ₃ -SCR catalyst. Catalysis Science and Technology, 2014, 4, 2932-2937.	4.1	27
104	The Effect of Hydrogen on the Storage of NOx Over Silver, Platinum and Barium Containing NSR Catalysts. Catalysis Letters, 2014, 144, 1101-1112.	2.6	4
105	Chemical deactivation by phosphorous under lean hydrothermal conditions over Cu/BEA NH3-SCR catalysts. Applied Catalysis B: Environmental, 2014, 147, 251-263.	20.2	45
106	Kinetic modeling of NOx storage and reduction using spatially resolved MS measurements. Applied Catalysis B: Environmental, 2014, 147, 1028-1041.	20.2	22
107	DME, propane and CO: The oxidation, steam reforming and WGS over Pt/Al2O3. The effect of aging and presence of water. Applied Catalysis B: Environmental, 2014, 160-161, 480-491.	20.2	19
108	The influence of hydrogen on the stability of nitrates during H2-assisted SCR over Ag/Al2O3 catalysts – A DRIFT study. Journal of Catalysis, 2013, 307, 153-161.	6.2	35

#	Article	IF	CITATIONS
109	Interzeolite Conversion of FAU Type Zeolite into CHA and its Application in NH3-SCR. Topics in Catalysis, 2013, 56, 550-557.	2.8	44
110	Enhanced Low Temperature NO x Reduction Performance Over Bimetallic Pt/Rh–BaO Lean NO x Trap Catalysts. Topics in Catalysis, 2013, 56, 68-74.	2.8	6
111	Influence of Hydrothermal Ageing on NH3-SCR Over Fe-BEA—Inhibition of NH3-SCR by Ammonia. Topics in Catalysis, 2013, 56, 80-88.	2.8	16
112	Characterization of Active Species in Cu-Beta Zeolite by Temperature-Programmed Reduction Mass Spectrometry (TPR-MS). Topics in Catalysis, 2013, 56, 201-204.	2.8	12
113	Investigation of the Effect of Accelerated Hydrothermal Aging on the Cu Sites in a Cu-BEA Catalyst for NH3-SCR Applications. Topics in Catalysis, 2013, 56, 317-322.	2.8	48
114	Hydrothermal Aging-Induced Changes in Washcoats of Commercial Three-Way Catalysts. Topics in Catalysis, 2013, 56, 323-328.	2.8	17
115	Sulfur Dioxide Exposure: A Way To Improve the Oxidation Catalyst Performance. Industrial & Engineering Chemistry Research, 2013, 52, 14556-14566.	3.7	24
116	A kinetic model of the hydrogen assisted selective catalytic reduction of NO with ammonia over Ag/Al ₂ O ₃ . AICHE Journal, 2013, 59, 4325-4333.	3.6	8
117	The effect of the gas composition on hydrogen-assisted NH3-SCR over Ag/Al2O3. Applied Catalysis B: Environmental, 2013, 136-137, 168-176.	20.2	26
118	Mechanistic investigations of the promoting role of Rh on the NSR performance of NOx storage BaO-based catalysts. Applied Catalysis B: Environmental, 2013, 132-133, 266-281.	20.2	16
119	Improved low-temperature SCR activity for Fe-BEA catalysts by H2-pretreatment. Applied Catalysis B: Environmental, 2013, 138-139, 373-380.	20.2	59
120	Experimental evidence of the mechanism behind NH3 overconsumption during SCR over Fe-zeolites. Journal of Catalysis, 2013, 299, 101-108.	6.2	38
121	The effect gas composition during thermal aging on the dispersion and NO oxidation activity over Pt/Al2O3 catalysts. Applied Catalysis B: Environmental, 2013, 129, 517-527.	20.2	65
122	Kinetic modeling of H-BEA and Fe-BEA as NH3-SCR catalysts—Effect of hydrothermal treatment. Catalysis Today, 2012, 197, 24-37.	4.4	56
123	Hydrothermal Stability of Fe–BEA as an NH ₃ -SCR Catalyst. Industrial & Engineering Chemistry Research, 2012, 51, 12762-12772.	3.7	79
124	Local ammonia storage and ammonia inhibition in a monolithic copper-beta zeolite SCR catalyst. Applied Catalysis B: Environmental, 2012, 126, 144-152.	20.2	31
125	Study of the "Fast SCR―like mechanism of H2-assisted SCR of NOx with ammonia over Ag/Al2O3. Applied Catalysis B: Environmental, 2012, 113-114, 228-236.	20.2	47
126	Mechanistic investigation of hydrothermal aging of Cu-Beta for ammonia SCR. Applied Catalysis B: Environmental, 2011, , .	20.2	15

#	Article	IF	CITATIONS
127	Urea decomposition and HNCO hydrolysis studied over titanium dioxide, Fe-Beta and γ-Alumina. Applied Catalysis B: Environmental, 2011, 106, 273-279.	20.2	67
128	Reduction of NOx over a combined NSR and SCR system. Applied Catalysis B: Environmental, 2010, 98, 112-121.	20.2	56
129	Kinetic modeling of sulfur poisoning and regeneration of lean NOx traps. Applied Catalysis B: Environmental, 2010, 100, 31-41.	20.2	25
130	Heat of adsorption for NH3, NO2 and NO on Cu-Beta zeolite using microcalorimeter for NH3 SCR applications. Catalysis Today, 2010, 151, 237-243.	4.4	49
131	A Kinetic Model for the Selective Catalytic Reduction of NO _{<i>x</i>} with NH ₃ over an Feâ°'zeolite Catalyst. Industrial & Engineering Chemistry Research, 2010, 49, 39-52.	3.7	92
132	The beneficial effect of SO2 on platinum migration and NO oxidation over Pt containing monolith catalysts. Catalysis Today, 2009, 147, S290-S294.	4.4	32
133	Urea thermolysis studied under flow reactor conditions using DSC and FT-IR. Chemical Engineering Journal, 2009, 150, 544-550.	12.7	123
134	Detailed kinetic modeling of NH3 SCR over Cu-ZSM-5. Applied Catalysis B: Environmental, 2009, 92, 138-153.	20.2	117
135	Detailed kinetic modeling of NOx adsorption and NO oxidation over Cu-ZSM-5. Applied Catalysis B: Environmental, 2009, 87, 200-210.	20.2	100
136	The influence of the preparation procedure on the storage and regeneration behavior of Pt and Ba based NOx storage and reduction catalysts. Applied Catalysis B: Environmental, 2009, 88, 240-248.	20.2	38
137	Detailed Kinetic Modeling of NH ₃ and H ₂ O Adsorption, and NH ₃ Oxidation over Cu-ZSM-5. Journal of Physical Chemistry C, 2009, 113, 1393-1405.	3.1	94
138	A kinetic model for ammonia selective catalytic reduction over Cu-ZSM-5. Applied Catalysis B: Environmental, 2008, 81, 203-217.	20.2	213
139	Detailed kinetic modeling of NOxNOx storage and reduction with hydrogen as the reducing agent and in the presence of CO2 and H2O over a Pt/Ba/Al catalyst. Journal of Catalysis, 2008, 258, 273-288.	6.2	66
140	Kinetic modelling of sulfur deactivation of Pt/BaO/Al2O3 and BaO/Al2O3 NOx storage catalysts. Applied Catalysis B: Environmental, 2007, 70, 179-188.	20.2	26
141	A kinetic study of NOx reduction over Pt/SiO2 model catalysts with hydrogen as the reducing agent. Topics in Catalysis, 2007, 42-43, 83-89.	2.8	10
142	Fundamental studies of NOx storage at low temperatures. Topics in Catalysis, 2007, 42-43, 95-98.	2.8	24
143	Identification of adsorbed species on Cu-ZSM-5 under NH3 SCR conditions. Topics in Catalysis, 2007, 42-43, 113-117.	2.8	80
144	Global Kinetic Modelling of a Supplier Barium- and Potassium-Containing Lean NOxTrap. Industrial & Engineering Chemistry Research, 2006, 45, 8883-8890.	3.7	20

#	Article	IF	CITATIONS
145	Selective catalytic reduction of NOx with NH3 over Cu-ZSM-5—The effect of changing the gas composition. Applied Catalysis B: Environmental, 2006, 64, 180-188.	20.2	225
146	Sulfur deactivation of Pt/SiO2, Pt/BaO/Al2O3, and BaO/Al2O3 NOx storage catalysts: Influence of SO2 exposure conditions. Journal of Catalysis, 2005, 234, 206-218.	6.2	44
147	Global Kinetic Model for Lean NOx Traps. Industrial & Engineering Chemistry Research, 2005, 44, 3021-3032.	3.7	93
148	Kinetic Modelling in Automotive Catalysis. Topics in Catalysis, 2004, 28, 89-98.	2.8	34
149	The Effect of a Changing Lean Gas Composition on the Ability of NO ₂ Formation and NO _x Reduction over Supported Pt Catalysts. Topics in Catalysis, 2004, 30/31, 85-90.	2.8	40
150	Mean field modelling of NOx storage on Pt/BaO/Al2O3. Catalysis Today, 2002, 73, 263-270.	4.4	110
151	A Kinetic Study of NO Oxidation and NOx Storage on Pt/Al2O3 and Pt/BaO/Al2O3. Journal of Physical Chemistry B, 2001, 105, 6895-6906.	2.6	318
152	Model Studies of NOx Storage and Sulphur Deactivation of NOx Storage Catalysts. Topics in Catalysis, 2001, 16/17, 133-137.	2.8	80
153	The mechanism for NOx storage. Catalysis Letters, 2000, 66, 71-74.	2.6	205
154	A Kinetic Study of Oxygen Adsorption/Desorption and NO Oxidation over Pt/Al2O3 Catalysts. Journal of Physical Chemistry B, 1999, 103, 10433-10439.	2.6	179
155	Performance Studies and Correlation between Vehicle- and Rapid- Aged Commercial Lean NOx Trap Catalysts. SAE International Journal of Engines, 0, 10, 1613-1626.	0.4	16
156	Effect of DMSO on the catalytical production of 2,5-bis(hydoxymethyl)furan from 5-hydroxymethylfurfural over Ni/SiO2 catalysts. Reaction Chemistry and Engineering, 0, , .	3.7	9
157	Investigation of CO Deactivation of Passive NOx Adsorption on La Promoted Pd/BEA. Emission Control Science and Technology, 0, , 1.	1.5	0